NeuroImage 299 (2024) 120843

Contents lists available at ScienceDirect

NeuroImage

journal homepage: www.elsevier.com/locate/ynimg

Olfaction modulates cortical arousal independent of perceived odor intensity and pleasantness

Fangshu Yao [a,b,c], Xiaoyue Chang [a,b], Bin Zhou [a,b,*], Wen Zhou [a,b,d,*]

[a] State Key Laboratory of Brain and Cognitive Science, Institute of Psychology, Chinese Academy of Sciences, Beijing 100101, China
[b] Department of Psychology, University of Chinese Academy of Sciences, Beijing 100049, China
[c] School of Psychology, Shanghai University of Sport, Shanghai 200438, China
[d] Chinese Institute for Brain Research, Beijing 102206, China

ARTICLE INFO

Keywords:
Odor
Arousal
Pupillary response
Alpha oscillations
Small-worldness
Attentional blink

ABSTRACT

Throughout history, various odors have been harnessed to invigorate or relax the mind. The mechanisms underlying odors' diverse arousal effects remain poorly understood. We conducted five experiments (184 participants) to investigate this issue, using pupillometry, electroencephalography, and the attentional blink paradigm, which exemplifies the limit in attentional capacity. Results demonstrated that exposure to citral, compared to vanillin, enlarged pupil size, reduced resting-state alpha oscillations and alpha network efficiency, augmented beta-gamma oscillations, and enhanced the coordination between parietal alpha and frontal beta-gamma activities. In parallel, it attenuated the attentional blink effect. These effects were observed despite citral and vanillin being comparable in perceived odor intensity, pleasantness, and nasal pungency, and were unlikely driven by semantic biases. Our findings reveal that odors differentially alter the small-worldness of brain network architecture, and thereby brain state and arousal. Furthermore, they establish arousal as a unique dimension in olfactory space, distinct from intensity and pleasantness.

1. Introduction

Odors act as emotional catalysts and have been used across cultures and throughout history for hedonistic purposes (Pybus, 2006). We turn to the scents of chamomile, orange blossom, and sandalwood, among others, in search of relaxation, refreshment, and tranquility. Our emotional responses to odors are partially innate and universal (Arshamian et al., 2022; Soussignan et al., 1997), and can even occur during sleep (Arzi et al., 2012; Schredl et al., 2009). This intimate association between odors and emotion is generally attributed to the anatomical overlap between the olfactory system and the limbic brain (Gottfried, 2010), particularly the amygdala — a central hub for emotion processing (Pessoa, 2017). Nonetheless, the exact underlying mechanisms are elusive.

It is commonly accepted that the basic structure of emotional experiences is two-dimensional: with the axes being valence and arousal (Russell, 1980). Valence is an assessment of one's current condition (pleasure-displeasure). Arousal — a state of mobility and energy — is a continuum of alertness that ranges from sleep to extreme excitement (Russell, 2003). On the other hand, the structure of olfactory space is less clear (Endo and Kazama, 2022; Secundo et al., 2014; Zhou et al., 2018). However, its primary axis seems to be valence (pleasant-unpleasant) as well (Secundo et al., 2014). Another prominent dimension is odor intensity, which depends on the Hill exponent of an odorant and its concentration (Mainland et al., 2014). Two decades ago, Bensafi and colleagues reported that odor intensity strongly correlates with both subjective state of arousal (as an effect of odor exposure) and skin conductance variations (Bensafi et al., 2002). Intensity has since been viewed as a surrogate for arousal in olfaction (Anderson et al., 2003; Jin et al., 2015; Winston et al., 2005). Several studies have exploited odorants whose intensity can be dissociated from pleasantness to disentangle the representations of affective valence and arousal in the amygdala and other associated regions. The findings have been inconsistent (Anderson et al., 2003; Jin et al., 2015; Winston et al., 2005). Some recent studies (Baccarani et al., 2021a; Chrea et al., 2009) have argued that odor-evoked affective experiences are multidimensional and cannot be adequately captured by bidimensional models. Moreover, stimulating and relaxing could be separate dimensions rather than the

* Corresponding authors.
E-mail addresses: zhoub@psych.ac.cn (B. Zhou), zhouw@psych.ac.cn (W. Zhou).

https://doi.org/10.1016/j.neuroimage.2024.120843
Received 2 May 2024; Received in revised form 22 August 2024; Accepted 6 September 2024
Available online 7 September 2024

opposite ends of a single arousal dimension.

While valence is intricately linked to external sensory events (stimuli) (Miskovic and Anderson, 2018), arousal is an internal state that is closely tied to autonomic responses, global brain activity, and attention (Flavell et al., 2022; Harris and Thiele, 2011; Lee and Dan, 2012; Marrocco et al., 1994). The arousal-related effects of different fragrances on the mind, whether calming, soothing, reviving, or invigorating, have particularly fascinated humans since ancient times and remain poorly understood, attracting continued research efforts (Baccarani et al., 2021a, 2021b; Cereghetti et al., 2024; Pybus, 2006). We sought to investigate whether and how odors differentially affect brain state and attention, and to evaluate whether these effects transcend the perceptual attributes of odor intensity and pleasantness. To this end, we combined pupillometry (Joshi and Gold, 2020; Mathot, 2018), electroencephalography (EEG), and the attentional blink paradigm (Shapiro et al., 1997), known to exemplify the limit in attentional capacity, to assess the effects of citral and vanillin on odor recipients. Citral is an acyclic monoterpene aldehyde with a lemon-like odor. Vanillin is a phenolic aldehyde of the same molecular weight (both 152 g mol^{-1}), and has a vanilla-like odor. Their respective odors have been suggested to be implicitly associated with different energizing/relaxing feelings (Lemercier-Talbot et al., 2019). In a series of experiments, we carefully matched citral and vanillin for perceived odor intensity and pleasantness, and systematically examined their impacts on pupil size, neural oscillatory profiles and connectivity patterns, and the magnitude and dynamics of the attentional blink.

2. Results

2.1. Odors alter pupil size independent of olfactory intensity and pleasantness

Pupil size provides a window into the inner workings of the brain. In addition to light, fixation, and eye movement, pupil size is modulated by non-visual factors such as attention and mental effort. Furthermore, it covaries with activity in the locus coeruleus, which governs global arousal (Joshi and Gold, 2020; Mathot, 2018). In Experiment 1, we collected pupillary responses from 40 normosmic participants following exposures to citral and vanillin. We recruited only women due to their generally superior olfactory and emotional sensitivities (Brand and Millot, 2001; Brody and Hall, 2008). Upon arrival, each participant was asked to select from a series of five citral solutions (0.01 %, 0.02 %, 0.03 %, 0.04 %, and 0.05 % v/v in propylene glycol) the one that best matched a target vanillin solution (14.5% m m^{-1} in propylene glycol) in terms of odor intensity and pleasantness. The vanillin solution and the chosen concentration of citral solution were used in the formal testing of that participant, which included an odor evaluation session followed by pupil measurements. Specifically, pupil size was tracked in four ~2-minute blocks with a break of at least one minute between blocks to eliminate olfactory adaptation. In each block, participants fixated on a central cross on a dark background while continuously inhaling through two nosepieces and exhaling through the mouth (Fig. 1A). Air was presented for the first minute (baseline) of each block, after which it was switched to either citral or vanillin. The order of the citral and vanillin blocks was counterbalanced across participants.

Overall, participants perceived citral and vanillin as equally intense and pleasant (mean ± SD: 3.3 ± 1.4 vs. 2.9 ± 1.5 and 4.1 ± 1.2 vs. 4.0 ± 1.3, $ts_{39} = 1.30$ and 0.31, ps = 0.20 and 0.76, $BFs_{10} = 0.28$ and 0.13, respectively), but subjectively felt that citral was more arousing than vanillin (3.5 ± 1.2 vs. 2.4 ± 1.1, $t_{39} = 4.87$, $p < 0.001$, Cohen's $d = 0.77$) (Fig. 1B). Fig. 1C shows the baseline-normalized pupillary responses in the 30 s following the switch of air to citral or vanillin (0–29 s). Compared to vanillin, exposure to citral significantly enlarged pupil size over this relatively long period ($t_{39} = 2.51$, $p = 0.016$, Cohen's $d = 0.40$). Closer inspection of the temporal dynamics of the pupillary responses revealed a significant effect of odor from 6 to 23 s following odor

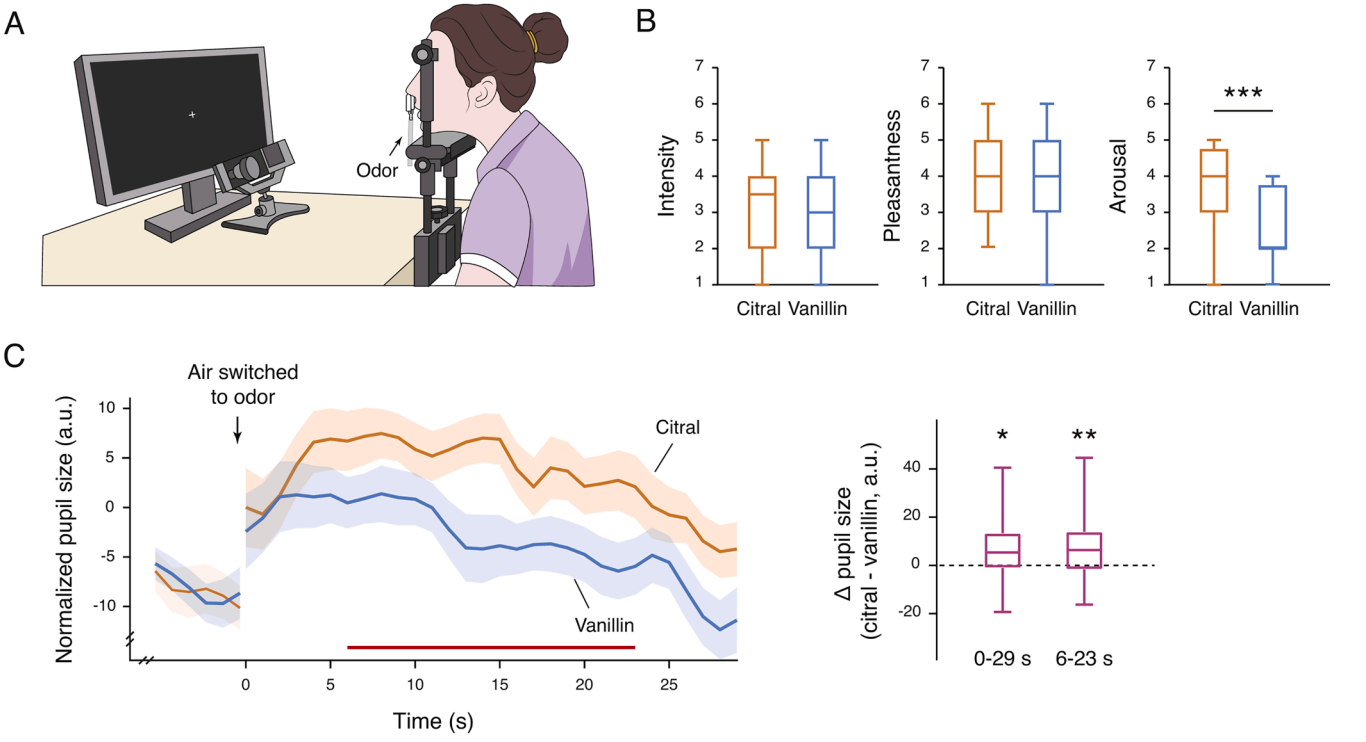

Fig. 1. Experiment 1: Olfactory modulation of pupil size. (A) Pupillometry setup. (B) Ratings of perceived odor intensity, pleasantness, and arousal for citral and vanillin. (C) Dynamics of baseline-normalized pupillary changes following the switch (at time 0) from air to either citral or vanillin (left), and the differences between conditions in mean pupil size over 0–29 s and 6–23 s. The red horizontal bar denotes significant consecutive time points between conditions (6–23 s). Shaded areas: SEMs. In each box and whisker plot, the central line denotes the median, the bottom and top edges of the box indicate the 25th and 75th percentiles, and the ends of the whiskers represent the 5th and 95th percentiles. *: $p < 0.05$, **: $p < 0.01$, ***: $p < 0.001$.

exposure (permutation test, cluster $p = 0.008$), where the pupil was more dilated in the presence of citral as opposed to vanillin ($t_{39} = 2.90$, $p = 0.006$, Cohen's $d = 0.46$). This effect was comparable between those who chose the lowest concentration of citral (0.01 v/v in propylene glycol) as the one that best matched the vanillin solution and those who selected higher citral concentrations (0–29 s: $t_{38} = 0.29$, $p = 0.77$, $BF_{10} = 0.25$; 6–23 s: $t_{38} = 0.32$, $p = 0.75$, $BF_{10} = 0.25$). It was also comparable between those who judged citral as more arousing than vanillin and those who did not (0–29 s: $t_{20.8} = 0.093$, $p = 0.93$, $BF_{10} = 0.24$; 6–23 s: $t_{20.4} = -0.16$, $p = 0.87$, $BF_{10} = 0.24$), and thus could not be accounted for by expectation or top-down control. Rather, the relatively sustained pupil changes likely reflected a combination of olfactory processing (processing of the odors of citral and vanillin) and odor-induced alteration of overall arousal and brain state (Joshi and Gold, 2020; Mathot, 2018). The latter could presumably be associated with a modification of the tonic discharge rates in the locus coeruleus.

2.2. Odors alter oscillatory brain activities independent of olfactory intensity and pleasantness

Brain states are defined by the dynamics of network activities on a timescale of seconds or more, and can be characterized by oscillatory fluctuations in EEGs (Harris and Thiele, 2011). In Experiment 2, we recruited an additional 40 women to examine the impacts of citral and vanillin on the patterns of scalp EEGs. We conducted resting-state recording to reveal the brain's ongoing intrinsic activity without the effects of complex stimuli (other than the odors used) or tasks. In each block, participants were asked to fixate on a central cross while being continuously exposed to either citral or vanillin (one odor per block) for a duration of 3 min. A 3-minute break was provided between blocks. As in Experiment 1, citral and vanillin were individually matched beforehand in terms of perceived intensity and pleasantness, and were rated by participants to be similarly intense and pleasant (3.9 ± 0.9 vs. 3.8 ± 1.1 and 5.0 ± 1.0 vs. 4.7 ± 0.9, $ts_{39} = 0.31$ and 1.59, $ps = 0.76$ and 0.12, $BFs_{10} = 0.13$ and 0.41, respectively; Fig. 2A). The order of the citral and vanillin blocks was balanced across participants.

As an initial step to quantify the impacts of odors on brain state, we extracted and compared the global power spectrum of neural oscillations in the range of 4 to 45 Hz when exposed to citral and vanillin, respectively. This encompassed theta (4–8 Hz), alpha (8–13 Hz), and beta (15–30 Hz) to low gamma (30–45 Hz) rhythms that underlie resting-state networks, reflecting the dynamical capabilities of the brain (Brookes et al., 2011; Deco et al., 2013; Mantini et al., 2007). We were particularly interested in alpha oscillations, which are tightly associated with arousal and attention (Klimesch, 2012; Mantini et al., 2007; Palva and Palva, 2007; Schubring and Schupp, 2021), as well as fast oscillations in the beta to low gamma range (Palva and Palva, 2007; Steriade, 2006). The physical architecture of neuronal networks dictates that

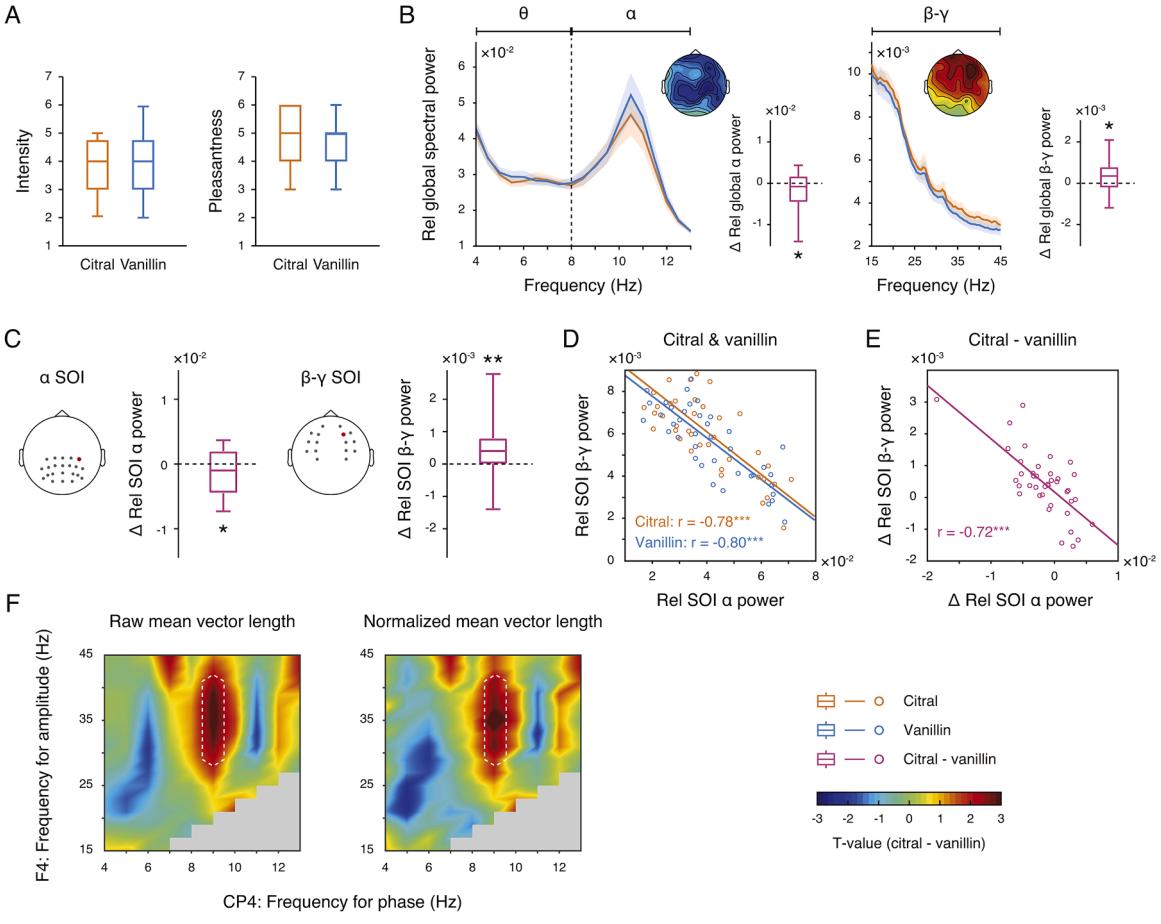

Fig. 2. Experiment 2: Olfactory modulation of oscillatory brain activities at rest. (A) Ratings of perceived odor intensity and pleasantness for citral and vanillin. (B) Relative global spectral powers for rhythmic activities in the theta, alpha, and beta-gamma bands under exposures to citral and vanillin. Insets show the differences between conditions in global alpha and beta-gamma powers and the corresponding topographical distributions. Shaded areas: SEMs. (C) Sensors of interest (SOIs) for alpha and beta-gamma activities and the differences between conditions in alpha and beta-gamma powers within the respective SOIs. Red dots: electrodes CP4 and F4. (D-E) Scatterplots of alpha and beta-gamma powers within the respective SOIs when exposed to citral and vanillin (D), and their differences between conditions (E). Each circle represents a participant. (F) Differences between conditions in the strength of phase-amplitude coupling between slow oscillatory activities recorded from CP4 and fast oscillatory activities recorded from F4, as indexed by the original and normalized mean vector length values (smoothed for display purposes). Dashed ellipses denote significant clusters between conditions. Box and whisker plots are as in Fig. 1. *: $p < 0.05$, **: $p < 0.01$, ***: $p < 0.001$.

alterations at slow frequencies (e.g., alpha) can lead to a cascade of energy dissipation at higher frequencies and modulate faster events (Buzsaki and Draguhn, 2004). Indeed, results (Fig. 2B) showed decreased global alpha oscillations (band power: $t_{39} = -2.18$, $p = 0.036$, Cohen's $d = 0.34$; peak power: $t_{39} = -2.29$, $p = 0.027$, Cohen's $d = 0.36$) and increased beta-gamma oscillations (band power: $t_{39} = 2.18$, $p = 0.035$, Cohen's $d = 0.35$) in the presence of citral compared to vanillin, with no difference in the theta band between the two odor conditions ($t_{39} = -0.67$, $p = 0.51$, $BF_{10} = 0.15$). The odor effects (citral vs. vanillin) tended to be right-lateralized and were largely distributed over central-parietal areas for oscillatory activities in the alpha band and across frontal regions for those in the beta-gamma band (Fig. 2B insets). We also examined beta and gamma oscillations separately, and found that they were similarly modulated by odors (citral vs. vanillin) in terms of both band power ($ts_{39} = 1.79$ and 2.42, $ps = 0.082$ and 0.021, Cohen's $ds = 0.28$ and 0.38, for beta and gamma oscillations, respectively) and spatial distribution of the odor effect (Figure S1). Taken together, these patterns point to a state of heightened vigilance and attention (Laufs et al., 2006) induced by citral relative to vanillin.

Considering that oscillatory dynamics coordinate communications between various neural assemblies (Palva and Palva, 2007; Siebenhuhner et al., 2020), we selected central-posterior and lateral-frontal scalp electrodes as the sensors of interest (SOIs) for alpha and beta-gamma activities, respectively (Fig. 2C). The alpha SOIs covered the visual and dorsal attentional resting-state networks, while the beta-gamma SOIs covered the lateralized frontoparietal resting-state networks (Brookes et al., 2011; Mantini et al., 2007). Analyses based on these SOIs recapitulated the distinct impacts of citral and vanillin on the strengths of oscillatory activities in the alpha and beta-gamma bands, and showed numerically larger odor effects ($ts_{39} = -2.39$ and 2.78, $ps = 0.022$ and 0.008, Cohen's $ds = 0.38$ and 0.44, respectively; Fig. 2C). Across participants, a strong negative correlation was observed between alpha power and beta-gamma power in the SOIs, irrespective of the odor condition ($rs = -0.78$ and -0.80, $ps < 0.001$, for citral and vanillin, respectively; Fig. 2D). This correlation hinted at inherent interareal interactions that could support attentional modulations of neuronal information transfer (Hyafil et al., 2015; Siegel et al., 2012; Womelsdorf et al., 2014). Moreover, such interareal interactions appeared to partially mediate the effects of odors on brain state — the difference in alpha power in the presence of citral versus vanillin was also significantly and negatively correlated with that in beta-gamma power ($r = -0.72$, $p < 0.001$, Fig. 2E).

In an effort to probe the oscillatory signature of olfactory influence on communications between the central-posterior and lateral-frontal areas of the brain, we compared the coupling strengths, as indexed by the mean vector length (Ozkurt and Schnitzler, 2011), between slow oscillatory activities (4–13 Hz) recorded from CP4 and fast oscillatory activities (15–45 Hz) recorded from F4 when exposed to citral and vanillin. We chose these two electrodes from the SOIs because they exhibited the most prominent odor effects on spectral powers for the alpha (CP4: $t_{39} = -2.77$, $p = 0.009$, Cohen's $d = 0.44$) and beta-gamma (F4: $t_{39} = 3.43$, $p = 0.001$, Cohen's $d = 0.54$) bands, respectively (Fig. 2B and C). As shown in Fig. 2F, odors significantly modulated the coupling strength between the phase time series of alpha oscillations (8–10 Hz) at CP4 and the amplitude envelopes of rhythmic activities in the high-beta low-gamma band (30–40 Hz) at F4, with a stronger coupling in the presence of citral compared to vanillin (raw mean vector length and normalized mean vector length, cluster-based permutation test $ps < 0.05$). This olfactory modulation of interareal cross-frequency phase-amplitude coupling was not a spurious artifact related to non-sinusoidal signals in neuronal activity (Siebenhuhner et al., 2020), as no odor effect on phase-amplitude coupling was observed for local oscillatory activities recorded at CP4 (Figure S2A) or F4 (Figure S2B). Rather, it suggested that odors genuinely modified the coordination between parietal alpha and frontal beta-gamma activities, in addition to modifying the strengths of these activities, of the brain at rest. Computationally, this empowers odors to exert a broad influence on information processing and cognition (Buzsaki and Draguhn, 2004; Hyafil et al., 2015; Palva and Palva, 2007), independent of olfactory intensity and pleasantness.

2.3. Odors alter functional brain connectivity independent of olfactory intensity and pleasantness

As the dominant rhythm in the human brain, alpha oscillations have been shown to subserve a specialized functional neural network organized by large-scale cortical phase-coupling (Engel et al., 2013; Vidaurre et al., 2018). The characteristics of phase-coupling in a frequency band are known to be susceptible to changes in the global brain state (Engel et al., 2013). This led to the question of whether odors would modify the functional organization of the alpha network. To address this, we calculated the pairwise phase consistency (PPC), a bias-free measure of the extent to which rhythmic signals generated by two separate sources display a consistent phase-relationship (synchronization) (Vinck et al., 2010). We did this for alpha activities across all combinations of electrode pairs when exposed to citral and vanillin, respectively. A comparison of the averaged PPCs across electrode pairs showed an overall reduced phase synchrony in the alpha band under exposure to citral relative to vanillin ($t_{39} = -2.22$, $p = 0.032$, Cohen's $d = 0.35$, Fig. 3A). The same analyses applied to signals in the theta and beta-gamma bands revealed no significant odor effect on global phase synchrony ($ts_{39} = -1.17$ and -0.014, $ps = 0.25$ and 0.99, $BFs_{10} = 0.24$ and 0.12, respectively; Fig. 3A).

Next, we used graph theory (Rubinov and Sporns, 2010) to investigate the influence of odors on network properties within the alpha band. We represented the alpha network under each odor condition as a graph, where nodes corresponded to different electrodes (cortical regions), and edges denoted the PPCs (functional connectivity) between electrodes. The connectivity matrices were subsequently thresholded to exclude weak or spurious connections and converted into binary undirected networks. We adopted 6 incremental values of PPC, from 0.1 to 0.6 in steps of 0.1, as cutoffs (Fig. 3B). Fig. 3C illustrates the odor-induced differences in functional connectivity at a PPC cutoff value of 0.1, primarily involving frontoparietal regions. At each threshold value, we extracted the following global and local connectivity measures (Latora and Marchiori, 2001; Watts and Strogatz, 1998) per odor condition: (1) Characteristic path length: the average of the minimum number of edges (shortest path length) between two nodes across all pairs of nodes. It indexes the typical separation between two nodes. (2) Global efficiency: the average inverse shortest path, primarily influenced by short rather than long paths. It reflects a network's overall efficiency for long-range information transfer. (3) Clustering coefficient: the ratio of the actual number of edges in the subgraph of the neighbors of a node (between the neighbors of that node) to the maximum possible number of edges in that subgraph, averaged across all nodes. It indexes the interconnectivity of a typical neighborhood. (4) Local efficiency: the average efficiency (inverse shortest path) of the local subgraphs. It reflects the extent to which a network is fault-tolerant. Collectively, these measures depict the small-world architecture of a network and are associated with the speed of signal propagation and the synchronizability within that network.

We conducted separate repeated-measures ANOVAs for these measures, using odor (citral vs. vanillin) and PPC threshold (0.1 to 0.6) as the within-subjects factors. The results demonstrated significant main effects of odor on characteristic path length and global efficiency ($Fs_{1, 39} = 5.38$ and 5.75, $ps = 0.026$ and 0.021, $\eta_p^2 s = 0.12$ and 0.13, respectively), regardless of the threshold value (odor × threshold: $ps \geq 0.1$) (Fig. 3D). A significant interaction was observed between odor and PPC threshold in clustering coefficient ($F_{2.76,\ 107.56} = 3.28$, $p = 0.027$, $\eta_p^2 = 0.077$), and a marginal interaction was found between them in local efficiency ($F_{2.13,\ 83.06} = 2.94$, $p = 0.055$), suggesting that the influence of odors on local connectivity depended on network density (Fig. 3E).

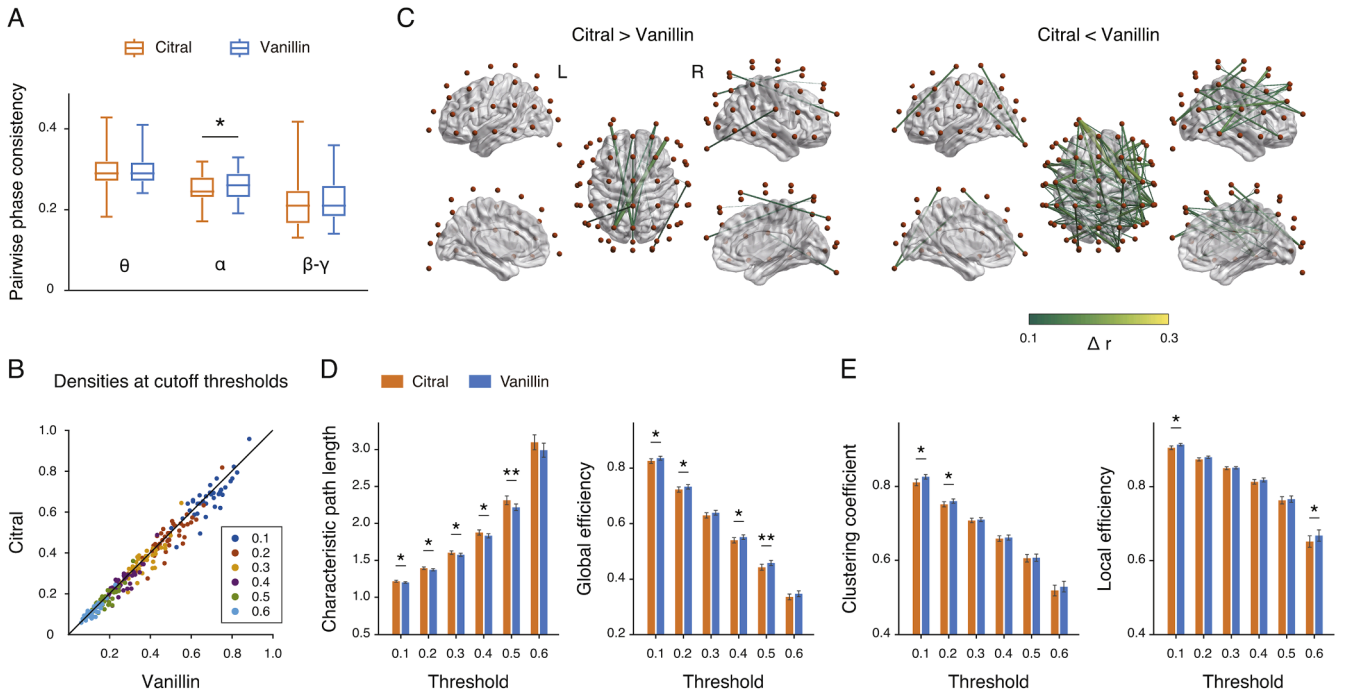

Fig. 3. Experiment 2: Olfactory modulation of the functional organization of the alpha network. (A) Global mean pairwise phase consistency (PPC) values for the theta, alpha, and beta-gamma bands. (B) Densities of the alpha network at PPC cutoff thresholds of 0.1 to 0.6 in steps of 0.1, under exposures to citral and vanillin. (C) Connectivity differences between conditions in the alpha network at a representative PPC threshold value of 0.1. Lines represent differential PPCs (Δ r) between electrodes (orange dots) that were larger than 0.1 when contrasting citral > vanillin and vanillin > citral. (D) Measurements of global connectivity in the alpha band across PPC thresholds when exposed to citral and vanillin. (E) Measurements of local connectivity in the alpha band across PPC thresholds when exposed to citral and vanillin. Error bars: SEMs. Box and whisker plots are as in Fig. 1. *: $p < 0.05$; **: $p < 0.01$.

Meanwhile, the main effects of odor for these two local connectivity measures were numerically evident but did not reach statistical significance ($Fs_{1,\ 39} = 3.52$ and 3.12, ps = 0.068 and 0.085, respectively; Fig. 3E). Conceptually, global efficiency and local efficiency are related to characteristic path length and clustering coefficient, respectively, and they measure how efficiently information is exchanged globally and locally over a network (Latora and Marchiori, 2001). To characterize the impact of odors on network efficiency, we entered the efficiency data into an omnibus repeated-measures ANOVA with odor, measure (global efficiency vs. local efficiency), and PPC threshold as the within-subjects factors. The ANOVA revealed a three-way interaction between these factors ($F_{2.69,\ 104.80} = 2.88$, $p = 0.045$, $\eta_p^2 = 0.069$), restating that the odor effects on global and local efficiencies had different dependencies on network density. Importantly, we observed a significant main effect of odor ($F_{1,\ 39} = 4.85$, $p = 0.034$, $\eta_p^2 = 0.11$), indicating that citral decreased the efficiency of the alpha network compared to vanillin. The same graph theory analyses with theta and beta-gamma bands showed no significant odor effect on network properties (Figure S3A and B).

Alpha oscillations and alpha band phase-couplings are implicated in inhibitory functions (Engel et al., 2013; Klimesch, 2012). The reduced efficiency of the alpha network when exposed to citral relative to vanillin, along with the reduced alpha band power and enhanced cross-frequency phase-amplitude coupling between parietal alpha and frontal beta-gamma activities, likely reflected a release from inhibition and conscious orienting (attentional investment) to and cognitive processing of environmental inputs (Klimesch, 2012).

2.4. *Independence of odor effects from semantic bias and odor trigeminality*

The observed effects in Experiment 2 could potentially be attributed to semantic associations. It is conceivable that the odors of citral and vanillin may activate the concepts of lemon and vanilla, respectively. These concepts could be semantically linked to varying levels of arousal (e.g., lemon is symbolic of freshness and energy). To explore this, we carried out Experiment 3, in which we replaced the odorants with their corresponding words, "lemon" and "vanilla", displayed at the center of the screen. Semantic processing of word meanings occurs automatically, even in the absence of attention (Deacon and Shelley-Tremblay, 2000), and the processing of odor-related words spontaneously evokes odor associations (Gonzalez et al., 2006). The experiment was otherwise identical to Experiment 2, but it yielded a different set of results.

Specifically, we found no significant influence of semantic label ("lemon" vs. "vanilla") on the strengths of global alpha (band power and peak power: $ts_{39} = 0.14$ and 0.93, ps = 0.89 and 0.36, $BFs_{10} = 0.12$ and 0.19, respectively), beta-gamma (band power: $t_{39} = -0.21$, $p = 0.83$, $BF_{10} = 0.13$), or theta (band power: $t_{39} = 0.39$, $p = 0.70$, $BF_{10} = 0.13$) activities (Fig. 4A). SOI-based analyses showed no difference in central-posterior alpha or lateral-frontal beta-gamma activities when participants viewed the words "lemon" versus "vanilla" (band powers: $ts_{39} = 0.49$ and 0.14, ps = 0.63 and 0.89, $BFs_{10} = 0.14$ and 0.12, respectively; Fig. 4B). Their powers remained inversely correlated across participants regardless of the condition (rs = −0.60 and −0.63, ps < 0.001; Fig. 4C). Additionally, the semantic labels did not differentially affect the phase-amplitude couplings between slow oscillatory activities at CP4 and fast oscillatory activities at F4 (Fig. 4D). In terms of phase synchrony within each frequency band, we observed no difference in mean PPC (averaged across all electrode pairs) between the two semantic conditions for alpha, theta, or beta-gamma oscillations ($ts_{39} = -0.37$, −0.23, and −0.59, ps = 0.71, 0.82 and 0.56, $BFs_{10} = 0.13$, 0.13, and 0.15, respectively; Fig. 4E). Graph theory analyses targeting the alpha network also showed no effect of semantic label on any of the network connectivity measures ($Fs_{1,\ 39} = 0.67$, 0.66, 0.38, and 0.77, ps = 0.42, 0.42, 0.54, and 0.39, for characteristic path length, global efficiency, clustering coefficient, and local efficiency, respectively) regardless of PPC threshold value (label × threshold: ps > 0.38) (Fig. 4F). Thus, semantic labels

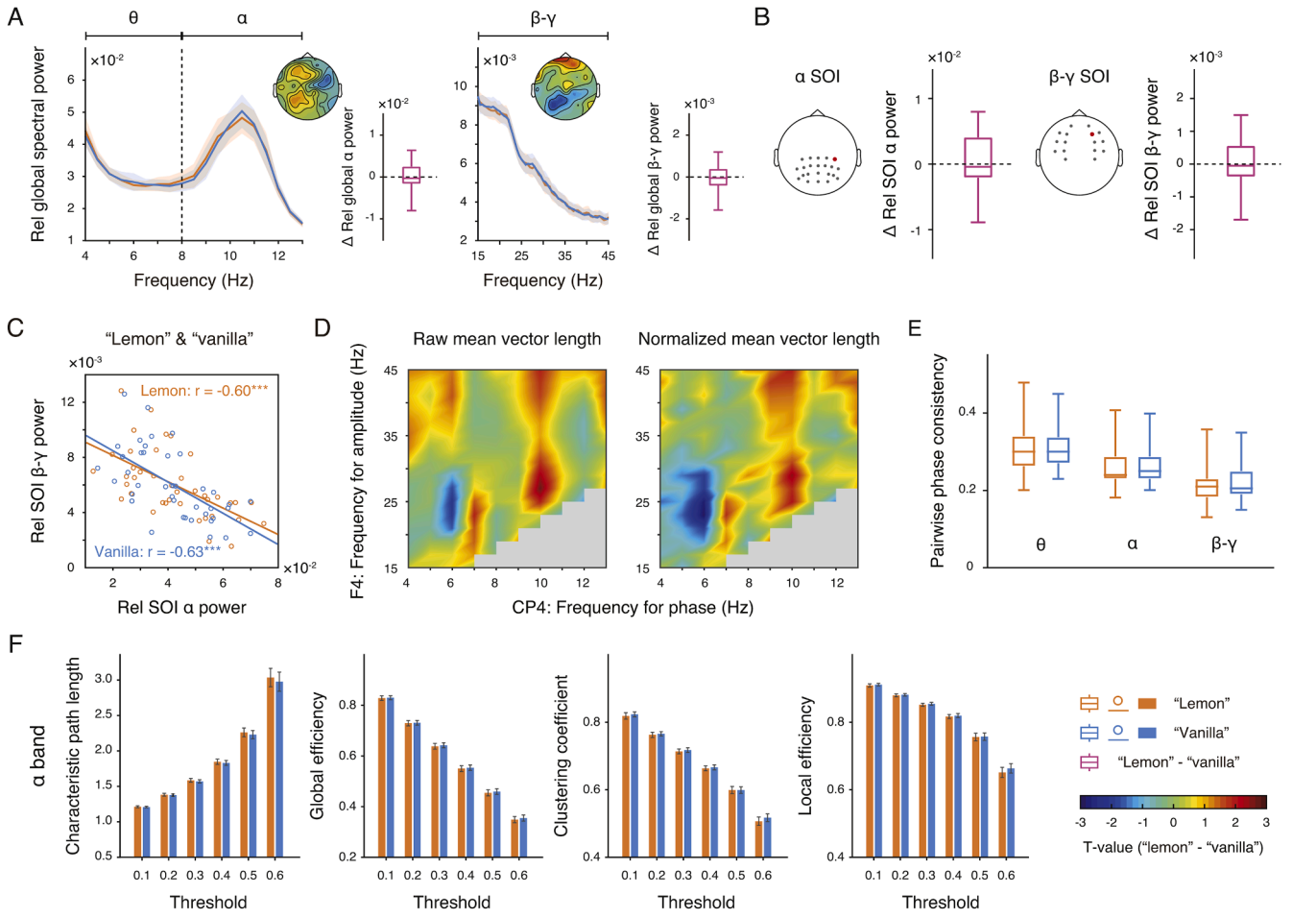

Fig. 4. Experiment 3: No significant effect of semantic labels on brain state at rest. (A) Relative global spectral powers for neural oscillations in the theta, alpha, and beta-gamma bands when viewing the words "lemon" and "vanilla". Insets show the differences between conditions in global alpha and beta-gamma powers and the corresponding topographical distributions. Shaded areas: SEMs. (B) Differences between conditions in alpha and beta-gamma powers within the respective SOIs. (C) Scatterplots of alpha and beta-gamma powers within the respective SOIs when viewing the words "lemon" and "vanilla". Each circle represents a participant. (D) Differences between conditions in the strength of phase-amplitude coupling between slow oscillatory activities recorded from CP4 and fast oscillatory activities recorded from F4, as indexed by the original and normalized mean vector length values (smoothed for display purposes). (E) Global mean PPC values for the theta, alpha, and beta-gamma bands. (F) Measurements of network connectivity in the alpha band across PPC thresholds when viewing the words "lemon" and "vanilla". Error bars: SEMs. Box and whisker plots are as in Fig. 1.

alone failed to modulate the power spectrum of oscillatory neural activities or interareal communications of the brain at rest.

We considered other possibilities: that the effects obtained in Experiments 1 and 2 were trigeminal rather than olfactory in nature (Jin et al., 2018), or that they could reflect a complex effect of odor familiarity or olfactory experience. Vanillin is known to be nontrigeminal (Doty et al., 1978); the concentrations of citral used in these experiments were low, no >0.05 % v/v in propylene glycol. However, one could argue that citral and vanillin may elicit different sensations of warmth, cold, itching, or tingling in the nose, which could result in varying levels of arousal. On the other hand, although odor familiarity does not appear to alter arousal levels in adults (Bensafi et al., 2002), familiar odors have been shown to exert a soothing effect on newborns (Goubet et al., 2007). Arguably, vanillin could be more familiar and hence less arousing than citral. To examine these alternatives, we recruited 24 women to complete two lateralization tasks (Wysocki et al., 2003) in Experiment 4. In one task, blindfolded participants received either citral (0.05 % v/v in propylene glycol, 8 trials) or vanillin (14.5% m m^{-1} in propylene glycol, 8 trials) in one nostril and air in the other (a blank jar). They were then asked to indicate whether the odor was presented to the left or right nostril (Figure S4A left). In the second task, they were dichorhinically presented with the two odorants — citral in one nostril and vanillin in the other nostril at the same time — and asked to identify which nostril smelled a more pungent or stimulating odor (8 trials, Figure S4B left). The participants also provided odor familiarity ratings for each of citral and vanillin. There was a break of at least 30 s between two trials.

We found that the lateralization accuracies were at chance for unilaterally presented citral as well as vanillin ($ts_{23} = -0.54$ and -0.37, $ps = 0.60$ and 0.72, $BFs_{10} = 0.18$ and 0.17, respectively; Figure S4A right). When the two odorants were dichorhinically presented, participants were equally likely to choose the nostril with citral and the nostril with vanillin as the side receiving a more pungent odor ($t_{23} = -1.03$, $p = 0.31$, $BF_{10} = 0.26$), that is, the choices were at chance (Figure S4B right). Hence, neither citral nor vanillin elicited trigeminal sensations at the concentrations used. Additionally, citral was perceived to be significantly more familiar than vanillin (5.8 ± 1.0 vs. 4.1 ± 1.6, $t_{23} = 4.97$, $p < 0.001$, Cohen's $d = 1.01$). As such, odor familiarity could not account for the heightened cortical arousal in the presence of citral relative to vanillin.

We therefore concluded that the different effects of citral and vanillin on pupil size and cortical oscillations, as observed in Experiments 1 and 2, were unlikely due to semantically mediated conceptual biases or to the odorants' trigeminal properties or familiarities. Instead, they manifested a genuine link between olfaction and arousal, independent of

perceived odor intensity and pleasantness.

2.5. Odors modulate magnitude and dynamics of attentional blink independent of olfactory intensity and pleasantness

Arousal sets the limit of attentional capacity, which in turn determines the extent to which a stimulus can be processed (Coull, 1998). Parameters of alpha oscillations have been associated with both pupil-linked arousal and attentional outcomes (Hanslmayr et al., 2011; MacLean et al., 2012; Stitt et al., 2018). In Experiment 5, we utilized the attentional blink paradigm, a well-established method for exposing the temporal constraint in information processing (Shapiro et al., 1997), to examine whether odors would differentially affect attentional performance. The demanding nature of this paradigm also eliminated the possibility of elaborate top-down processing of the semantic or episodic associations of the olfactory stimuli. Specifically, we invited 40 women to participate in a rapid serial visual presentation (RSVP) task (Fig. 5A) over two days. They completed 6 blocks per day, with each block performed under continuous exposure to either citral or vanillin, and a 3-minute break between blocks. As in Experiments 1 and 2, citral and vanillin were individually matched in advance for odor intensity and pleasantness, and were judged as equivalent in these perceptual attributes (4.5 ± 0.8 vs. 4.3 ± 1.1 and 4.9 ± 0.9 vs. 4.8 ± 0.7, $ts_{39} = 1.44$ and 0.92, ps = 0.16 and 0.36, $BFs_{10} = 0.33$ and 0.19, respectively; Fig. 5B). Each trial of the RSVP task began with a 2-s fixation cross, followed by an RSVP stream of 17 capital letters (8.6 items/s), which included 2 circled ones that served as the targets (T1 and T2) and 15 uncircled distractors, presented in a random order. Participants then reported the first and second targets (T1 and T2) in sequence. The interval between T1 and T2 ranged from 0 to 6 items (lag 1 to lag 7). Each block consisted of 42 trials, with 6 trials per lag. The order of odors was counterbalanced across days and participants.

Fig. 5C plots the identification accuracy for T1 and that for T2, contingent on correct responses for T1, under each odor condition as a function of the relative serial position of T2 (T1-T2 interval: lag 1 to lag 7). As is typical in an attentional blink effect, T2 accuracy was significantly below T1 accuracy at lags 1–5 (ps ≤ 0.021) and recovered at lags 6 and 7 (T2 accuracy vs. T1 accuracy: ps = 0.55 and 0.94, respectively). In other words, allocating attention to T1 limited the attentional resources available to process T2 when T2 was presented within approximately 500 ms following T1. While T1 accuracy was unaffected by odor condition ($t_{39} = -0.72$, $p = 0.48$, $BF_{10} = 0.16$), we found that T2 accuracy significantly improved under citral exposure relative to vanillin ($t_{39} = 2.27$, $p = 0.029$, Cohen's $d = 0.36$). In particular, smelling citral, compared to vanillin, significantly raised the lower limit of T2 accuracy (lowest T2 accuracy across all lags, $t_{39} = 2.92$, $p = 0.006$, Cohen's $d = 0.46$) and increased T2 accuracy at lag 5, the upper bound of the attention blink window ($t_{39} = 2.42$, $p = 0.020$, Cohen's $d = 0.38$), suggesting an attenuation of the attentional blink effect in terms of both magnitude and temporal extent. To further explore the odor effects, we quantified attentional blink magnitude as the proportional reduction in accuracy from the lag with the highest T2 accuracy to that with the lowest T2 accuracy. Additionally, for incorrect T2 reports in trials with correct T1 identifications, we calculated the proportions of reported items appearing after T2 (at a later serial position) and before T2 (at an earlier serial position), respectively, and used the difference between these proportions (after T2 – before T2) as an index of the extent to which temporal selection was delayed during the attentional blink (Vul et al., 2008). Comparisons between the two odor conditions revealed that the blink magnitude was 3.67 % smaller when exposed to citral compared to vanillin ($t_{39} = -2.49$, $p = 0.017$, Cohen's $d = 0.39$; Fig. 5D). Meanwhile, the temporal selection for T2 was also less delayed ($t_{39} = -2.21$, $p = 0.033$, Cohen's $d = 0.35$; Fig. 5E), corroborating the aforementioned overall enhancement of T2 accuracy.

Therefore, citral and vanillin exhibited differential effects on the limits and dynamics of attention in temporal selection independent of

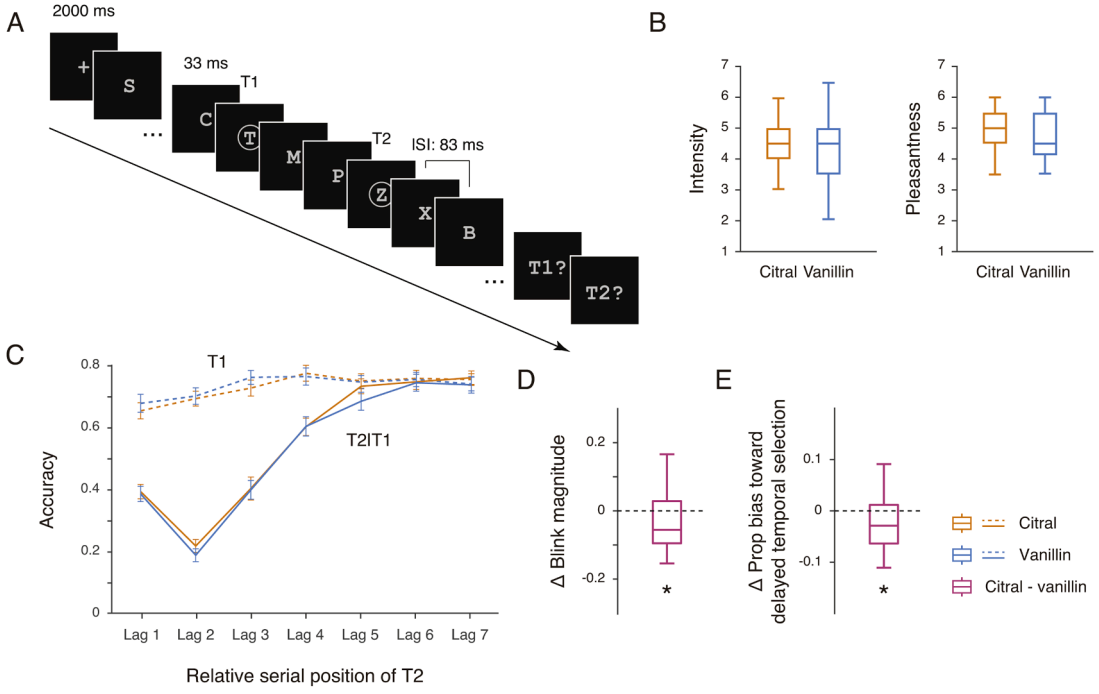

Fig. 5. Experiment 5: Olfactory modulation of the attentional blink effect. (A) Schematic illustration of the experimental paradigm. Each trial presented 17 letters in a random, non-repeating order. Two letters, encircled by a concurrently presented annulus, served as the targets T1 and T2. The serial position of T2 relative to T1 ranged from 1 (lag 1) to 7 (lag 7). Participants were asked to identify T1 and T2 in order. (B) Ratings of perceived odor intensity and pleasantness for citral and vanillin. (C) Identification accuracies for T1 (dashed lines) and T2 (solid lines, contingent on correct T1 responses) when exposed to citral and vanillin, plotted against the relative serial position of T2. Error bars: SEMs. (D-E) Differences between conditions in blink magnitude (D) and proportional bias toward delayed temporal selection (E). Box and whisker plots are as in Fig. 1. *: $p < 0.05$.

perceived odor intensity and pleasantness, in line with their differential impacts on arousal and brain state observed in Experiments 1 and 2.

3. Discussion

Lewis Thomas poetically writes (Thomas, 1990): "The act of smelling something, anything, is remarkably like the act of thinking itself. Immediately, at the very moment of perception, you can feel the mind going to work, sending the odor around from place to place, setting off complex repertoires throughout the brain …" Our data echo his descriptions of olfactory experiences and demonstrate that different odors exert differential effects on the global mind state, as manifested in pupil size, power spectrum of neural oscillations, functional brain connectivity, and the temporal limits and dynamics of attention. All neurophysiological and behavioral measures consistently show that odors induce varying levels of cortical arousal. These effects were obtained despite the odorants used being comparable in perceived intensity, pleasantness, and nasal pungency (trigeminality), and were unlikely driven by semantic biases. While our findings do not question the link between arousal and odor intensity (sensory magnitude) (Bensafi et al., 2002), they, along with other recent studies (Baccarani et al., 2021a, 2021b), challenge the simplified view that odor-induced arousal is identical or equivalent to the perceptual attribute of odor intensity. The privileged access of odors to the emotional system (the amygdala and other limbic structures) (Gottfried, 2010) does not fuse intensity and arousal into one dimension in the olfactory space.

The impacts of odors on human cortical oscillations were first observed over three decades ago (Lorig and Schwartz, 1988). Subsequent studies seeking to dissect their emotional effects have primarily focused on pleasantness (valence) and the different neural representations of odor pleasantness and intensity (Anderson et al., 2003; Jin et al., 2015; Secundo et al., 2014; Winston et al., 2005). How odors affect arousal beyond perceived intensity remains unclear. Our results indicate that this is mainly achieved through modifications of the strengths and network properties of alpha activities. Compared to vanillin, citral, which was perceived as equally intense and pleasant, decreased global oscillatory activities in the alpha band and desynchronized (dephased) alpha activities across the cortex, particularly in the frontoparietal regions. This perturbed the small-world architecture of the alpha network and reduced its neural efficiency. These changes were accompanied by augmented beta-gamma activities in the frontal regions and enhanced coordination (phase-amplitude coupling) between parietal alpha and frontal beta-gamma activities. The alpha rhythm is closely related to the default mode and attentional networks (Brookes et al., 2011; Mantini et al., 2007; Vidaurre et al., 2018). It has been theorized that alpha amplitude reflects the level of cortical inhibition, while the cross-frequency coupling between alpha and beta-gamma oscillations underpins attentional selection and a range of cognitive operations (Hyafil et al., 2015; Klimesch, 2012; Palva and Palva, 2007; Vidaurre et al., 2018; Womelsdorf et al., 2014). Thus, exposure to citral, relative to vanillin, seems to pull the resting-state networks into a functional configuration that mobilizes attentional resources for cognitive processing of external inputs, i.e., into a state with heightened arousal and vigilance (Deco et al., 2013). Concordantly, we observed an attenuation of the attentional blink effect under exposure to citral compared to vanillin, which implied an alleviation of the insufficiency of attentional resources (Hanslmayr et al., 2011; MacLean et al., 2012; Shapiro et al., 1997). Since we did not include an odorless control condition, it is unclear to what extent these effects were driven by citral being arousing, or vanillin being relaxing, or both. Additionally, more studies are needed to verify whether these effects generalize to other odors (e.g., eucalyptus oil and lavender oil) or reflect a generic olfactory modulation of arousal shared across different odors.

Several structures along the olfactory pathway, including the olfactory bulb, amygdala, and hypothalamus, project to locus coeruleus norepinephrine neurons (Schwarz et al., 2015). These neurons regulate core physiological and behavioral processes, as well as pupil motility (Joshi and Gold, 2020; Mathot, 2018). The locus coeruleus also innervates thalamocortical neurons, which play a critical role in the generation of the alpha rhythm (McCormick et al., 1991; Womelsdorf et al., 2014). We speculate that these interconnected circuits form the anatomical basis for the observed olfactory modulation of cortical arousal. The exact circuit mechanisms await future research.

Our results also indicate that arousal is, to a certain extent, an intrinsic property of odorants, rather than a derivative of perceived odor intensity or pleasantness. Indeed, there are many anecdotes about certain scents instilling a feeling of calmness, while others boost one's mood. This is reminiscent of colors: some hues (e.g., green-yellow) are more arousing than others (e.g., purple-blue) regardless of brightness and saturation (Valdez and Mehrabian, 1994). What structural or quality features contribute to an odorant's effect on arousal remain a mystery. The key may lie in the close links between olfaction and metabolism/homeostasis, the latter of which ultimately controls the level of arousal and governs the cortical network response state (Cunningham et al., 2006; Deco et al., 2013; Flavell et al., 2022; Jovanovic and Riera, 2022). Anatomically, the hypothalamus is well-positioned to serve as a central hub in the crosstalk between the olfactory system and the neurocircuits of energy homeostasis (Jovanovic and Riera, 2022).

4. Methods

4.1. Participants

Valid data were obtained from a total of 184 healthy female nonsmokers: 40 in Experiment 1 (mean age ± SD = 23.1 ± 0.9 yrs), 40 in Experiment 2 (21.8 ± 2.0 yrs), 40 in Experiment 3 (23.5 ± 2.8 yrs), 24 in Experiment 4 (23.0 ± 2.4 yrs), and 40 in Experiment 5 (22.6 ± 1.7 yrs). The participants were not aware of the experimental purposes. All participants reported having a normal sense of smell and no respiratory allergies or upper respiratory infections at the time of testing. All participants, except those in Experiment 4, also reported having normal or corrected-to-normal vision. They provided written informed consent to participate in procedures approved by the Institutional Review Board at the Institute of Psychology, Chinese Academy of Sciences.

4.2. Olfactory stimuli

The olfactory stimuli consisted of vanillin (14.5% m m^{-1}) and various concentrations of citral (0.01 %, 0.02 %, 0.03 %, 0.04 %, and 0.05 % v/v), both dissolved in propylene glycol. These stimuli were presented in identical 40 ml polypropylene jars, with each jar containing 10 ml of clear liquid. Each odor jar was fitted with either one Teflon nosepiece (in Experiment 4) or two (via a Y structure, in all other experiments). In Experiments 1, 2, 3, and 5, participants were asked beforehand to select from the citral solutions the one that best matched the vanillin solution in terms of odor intensity and pleasantness. The chosen concentration of the citral solution, along with the vanillin solution, was then used in the formal testing of that participant. In Experiment 4, the vanillin solution and the highest concentration (0.05 v/v) citral solution were used for odor trigeminality and familiarity assessments. Participants were instructed to inhale through the nosepieces and exhale through the mouth when smelling from the odor jars.

4.3. Visual stimuli

In Experiment 5, the rapid serial visual presentation (RSVP) streams each consisted of 17 different capital letters (Fig. 5A). These letters were presented successively in random order at the center of display. Each letter was displayed for 33 ms and was followed by an 83 ms blank, resulting in an RSVP rate of 8.6 items/s. The letters, in 40-point Courier New Bold font, were silver gray and subtended approximately 1.2° ×

1.2° on a black background. In each trial, two of the letters in the RSVP stream were encircled by a concurrently presented silver gray annulus (2.2° × 1.8°) and served as the targets (T1 and T2). T1 (the first annulus) appeared randomly in positions 3, 4, or 5 of the RSVP streams. The separation between T1 and T2 (the first and second annuli) was manipulated over 7 levels, ranging from 0 to 6 items (lag 1 to lag 7), which also occurred randomly.

4.4. Data acquisition

4.4.1. Behavioral procedures

Odor evaluation: Participants in Experiments 1, 2, and 5 undertook an odor evaluation task at the beginning of the formal testing. They were presented with citral (at a concentration individually selected by each participant) and vanillin, and were asked to rate the intensity and pleasantness of each odor on 7-point Likert scales. On these scales, 1 signified "extremely weak" and "neutral", while 7 indicated "extremely strong" and "extremely pleasant", respectively. Participants in Experiment 1 also provided ratings for the effect of each odor on their subjective state of arousal, using a 7-point Likert scale where 1 represented "not at all arousing" and 7 represented "extremely arousing". A minimum interval of 30 s was maintained between the samplings of the two odorants.

Odor lateralization and familiarity: Participants in Experiment 4 were tested for odor trigeminality and familiarity. To assess odor trigeminality, we employed two lateralization tasks (Wysocki et al., 2003). In the first task, participants were presented with either citral or vanillin in one nostril, and air (from a blank jar) in the other (Figure S4A left). They were then asked to indicate whether the odor was presented to the left or right nostril. Each odorant was tested in 4 trials per nostril, in a random order, totaling 16 trials (8 trials each for citral and vanillin). In the second task, participants were simultaneously presented with citral and vanillin, one in each nostril (Figure S4B left). They were asked to identify which nostril detected a more pungent or stimulating odor. There were 4 trials per combination of nostril and odorant, in a random order, totaling 8 trials. Participants were blindfolded during these tasks. For the assessment of odor familiarity, participants provided familiarity ratings for each of citral and vanillin on a 7-point Likert scale, where 1 represented "extremely unfamiliar" and 7 indicated "extremely familiar". To prevent olfactory fatigue, a break of at least 30 s was ensured between two trials.

Attentional blink: The RSVP task (Fig. 5A) in Experiment 5 was adapted from a previous study (Vul et al., 2008). Each trial began with a 2-s fixation cross, followed by an RSVP stream of 17 letters. This stream included 2 circled targets (T1 and T2) and 15 distractors in random order. The interval between T1 and T2 ranged from 0 to 6 items, resulting in 7 levels (lag 1 to lag 7). Participants were then prompted to select the letters corresponding to T1 and T2 in order from 6 different letters displayed on the screen. Among these 6 letters were the two targets and distractors preceding and following T2. The letter selected as T1 was subsequently replaced with a different random letter in the RSVP stream as one of the 6 choices for T2. The next trial started 0.3 s after a response was registered for T2. Each block consisted of 42 trials, with 6 trials per lag in random order, and was performed under the continuous exposure of either citral or vanillin. Participants completed a total of 12 blocks over two separate days (6 blocks per day, following the odor evaluation task). The order of citral and vanillin exposure was counterbalanced across days and participants. A break of 3 min was given between two blocks.

4.4.2. Pupillometry

In Experiment 1, pupil diameter was recorded monocularly in arbitrary pixels at 1000 Hz during four ~2-minute blocks, using an Eyelink 1000 Plus desktop mount eye tracker (SR Research Ltd, Canada). In each block, participants were instructed to fixate on a central cross (0.6° × 0.6°) on a dark background while continuously inhaling through two nosepieces and exhaling through the mouth (Fig. 1A). The nosepieces were connected to a Y structure (fixated on the chinrest) and a push-to-connect tube fitting. The tube fitting allowed for easy connection and disconnection to a jar, facilitating an easy switch from a blank jar to an odor jar during a block. Air (from a blank jar) was presented for the first minute (baseline) of each block, after which it was switched to either citral (2 blocks) or vanillin (2 blocks) by the experimenter, without interrupting the participant. The order of the citral and vanillin blocks was counterbalanced across participants. There was a break of at least one minute between two blocks.

4.4.3. EEG recordings

In Experiments 2 and 3, scalp EEGs were recorded using a 64-channel Neuroscan SynAmps^2 system (Compumedics NeuroScan). The sampling rate was set at 500 Hz and electrode impedance was kept below 5 KΩ. The signals were initially referenced online to an electrode between CZ and CPZ, and re-referenced offline to the average of both mastoids (M1 and M2). Horizontal and vertical eye movements were monitored by electrodes placed near the outer canthi of both eyes and electrodes positioned below and above the left eye, respectively.

In Experiment 2, resting-state EEGs were collected in a dark shielded room during two 3-minute blocks, with a 3-minute break in between. In each block, participants were instructed to fixate on a silver-gray central cross (1.1° × 1.1°) displayed on a black background. During this time, they were continuously exposed to either citral or vanillin, with one odorant per block. The order of odorant presentation was counterbalanced across participants. In Experiment 3, no odor was presented. Instead, participants viewed the word "lemon" or "vanilla" (3.2° × 1.5°, in Chinese), with one word displayed per block at the center of the screen. The procedure was otherwise identical to that in Experiment 2.

4.5. Data analyses

4.5.1. Behavioral analysis

Comparisons of odor ratings in Experiments 1, 2, and 5 were performed using the paired samples *t*-test. In Experiment 4, we compared both the lateralization accuracies for each odorant and the proportions of times an odorant was deemed more pungent during dichorhinic presentations against chance (0.5) using the one-sample *t*-test. For Experiment 5, we calculated the following measures for each participant per odor condition, based on the target identification accuracies at each lag: mean T1 accuracy, mean T2 accuracy, lower limit of T2 accuracy across all lags, T2 accuracy at lag 5 (the upper bound of the attention blink window), blink magnitude ($\frac{T2_{max}-T2_{min}}{T2_{max}}$, where $T2_{max}$ and $T2_{min}$ denote the upper and lower limits of T2 accuracy across all lags, respectively), and proportional bias toward delayed temporal selection (the difference between the proportions of reported items appearing after T2 and before T2, for incorrect T2 reports in trials with correct T1 identifications). T2 accuracies were contingent on correct responses for T1. We compared these measures between the two odor conditions using the paired samples *t*-test. The effect size for *t*-tests was estimated using Cohen's d. Bayes factors were estimated for tests with nonsignificant p-values. All tests were two-tailed.

4.5.2. Pupillometric analysis

Eye-blinks and other transient noises in the eye-tracking data were detected offline and subsequently removed using a linear interpolation algorithm (Kret and Sjak-Shie, 2019). The data were smoothed using a moving average filter with the span parameter set to 2 s and resampled at 1 Hz. The data were then normalized to the baseline by subtracting the average pupil diameter during the 1-minute baseline (air exposure) from all datapoints in that block. We focused on pupillary responses in the 30 s following the switch from air to either citral or vanillin (0–29 s), and compared the mean pupil diameter over this period between the two odor conditions using the paired samples *t*-test. To highlight the

different effects of odors on the temporal dynamics of pupillary changes, we quantified the differences in the mean pupil diameter between conditions within a sliding window of 5 s from 0 to 29 s following odor onset, with a step of 1 s. The differences were subjected to a cluster-based permutation test with 2000 randomizations.

4.5.3. EEG analysis

Preprocessing. EEG data were analyzed primarily with the MATLAB toolbox Fieldtrip (Oostenveld et al., 2011). To avoid potential noise caused by adjustments of nosepieces and postures at the beginning of a block, we removed EEG data recorded in the first 15 s of each block. The data were then segmented into 2-s epochs, demeaned, band-pass filtered from 0.5 to 100 Hz, and notch-filtered at 50 Hz. We applied independent component analysis to the segmented data to remove artefacts caused by eye blinks, muscle movements, or heartbeats. The resulting data were further visually inspected for artefacts. Channels with excessive noise were excluded on an individual basis.

Spectral analysis. We calculated spectral powers for frequencies from 1 to 100 Hz in each epoch using fast Fourier transformation with steps of 0.5 Hz, and averaged them across epochs for each condition and participant. We then converted the spectral powers for theta (4–8 Hz), alpha (8–13 Hz), beta (15–30 Hz), and low gamma (30–45 Hz) rhythms, which underlie resting-state networks (Brookes et al., 2011; Mantini et al., 2007), into relative powers by dividing them by the total energy from all of these bands. The average relative power of a band across all electrodes indexed the global strength of neural activities in that band. We also identified the peak frequency within the alpha range and extracted the peak power for each condition and participant. The relative global powers for theta, alpha, and beta-gamma activities, as well as the peak powers of alpha oscillations, were compared between conditions using the paired samples *t*-test.

In addition, we selected central-posterior (CP1, CP2, CP3, CP4, CPZ, P1, P2, P3, P4, P5, P6, PZ, PO3, PO4, PO5, PO6, PO7, PO8, POZ, O1, O2, and OZ; covering the visual and dorsal attentional resting-state networks) and lateral-frontal scalp electrodes (AF3, AF4, F3, F4, F5, F6, FC3, FC4, FC5, FC6, C3, C4, C5, C6, CP3, and CP4; covering the lateralized frontoparietal resting-state networks) as the sensors of interest for alpha and beta-gamma activities, respectively (SOIs, Fig. 2C) (Brookes et al., 2011; Mantini et al., 2007). We performed paired samples *t*-tests to compare the alpha and beta-gamma powers within the respective ROIs between conditions, and Pearson correlations to examine the relationships between the powers of central-posterior alpha and lateral-frontal beta-gamma activities across participants.

Phase-amplitude coupling analysis. Among the sensors of interest, CP4 and F4 exhibited the most prominent odor effects on spectral powers for the alpha and beta-gamma bands, respectively. We used the mean vector length to estimate phase-amplitude coupling between slow oscillatory activities (4–13 Hz in steps of 1 Hz) recorded from CP4 and fast oscillatory activities (15–45 Hz in steps of 2 Hz) recorded from F4 for each condition and participant. The value was calculated as $\frac{1}{\sqrt{N}}\frac{|\frac{1}{N}\sum_{n=1}^{N}A_h(n)e^{i(\phi_l(n))}|}{\sqrt{\frac{1}{N}\sum_{n=1}^{N}A_h(n)^2}}$, where N represents the number of time points, A_h the instantaneous amplitude of high-frequency oscillations, and ϕ_l the instantaneous phase of low-frequency activities (Ozkurt and Schnitzler, 2011). As a comparative control in Experiment 2, we also estimated the within-electrode phase-amplitude couplings for CP4 and F4, respectively.

Specifically, for each condition and participant, the mean vector length was calculated for each combination of low-frequency phase and high-frequency amplitude in individual epochs (data in the middle 1 s of each epoch was used for calculation, with the remaining data as padding) and then averaged across epochs. We constructed surrogate data set by shuffling epochs and phase information, and estimated the corresponding mean vector lengths for 200 repeats. The original mean vector length values were then normalized by subtracting the mean surrogate values. The original and normalized mean vector length values were compared between conditions using non-parametric cluster-based permutation tests with 2000 randomizations.

Graph theoretical analysis. For a given frequency band, the pairwise phase consistency (PPC) between rhythmic signals recorded at two separate electrodes was calculated as $PPC = \frac{2}{N(N-1)}\sum_{i=1}^{N-1}\sum_{j=(i+1)}^{N}f(\theta_i, \theta_j)$, where θ represents the relative phase between signals at two electrodes, N is the number of epochs, and $f(\theta_i, \theta_j)$ is defined by the cosine of the angular distance between vectors θ_i and θ_j (Vinck et al., 2010). For each condition and participant, the PPCs for all electrode pairs formed a connectivity matrix, with each cell (except the diagonal ones) representing the connectivity strength between signals of that frequency band at two electrodes. The connectivity matrices were then thresholded and converted into binary undirected networks. Graph theoretical analysis was conducted on these binary networks, with electrodes as nodes and thresholded PPCs (binary) as edges linking nodes, using the Brain Connectivity Toolbox (Rubinov and Sporns, 2010). We applied 6 different PPC thresholds: 0.1, 0.2, 0.3, 0.4, 0.5, and 0.6. At each threshold value, we extracted the following measures that depict the small-world architecture of a network: characteristic path length, global efficiency, clustering coefficient, and local efficiency (Latora and Marchiori, 2001; Watts and Strogatz, 1998). Separate repeated-measures ANOVAs were conducted for these measures, with condition and PPC threshold as the within-subjects factors.

CRediT authorship contribution statement

Fangshu Yao: Writing – review & editing, Writing – original draft, Visualization, Investigation, Formal analysis, Data curation. **Xiaoyue Chang:** Writing – original draft, Visualization, Investigation, Formal analysis, Data curation. **Bin Zhou:** Writing – review & editing, Writing – original draft, Visualization, Supervision, Methodology, Investigation, Funding acquisition, Formal analysis, Data curation, Conceptualization. **Wen Zhou:** Writing – review & editing, Writing – original draft, Visualization, Supervision, Methodology, Funding acquisition, Conceptualization.

Declaration of competing interest

The authors declare no competing interests.

Data availability

All reported data and analysis scripts are available at https://www.scidb.cn/en/s/uQBvYz.

Acknowledgements

This work was supported by STI2030-Major Projects 2021ZD0203100 (B.Z.) and 2021ZD0204200 (W.Z.), the Chinese Academy of Sciences Grant JCTD-2021-06 (W.Z.), and the National Natural Science Foundation of China (31671138) (B.Z.). The funders had no role in study design, data collection and analysis, decision to publish or preparation of the manuscript.

Supplementary materials

Supplementary material associated with this article can be found, in the online version, at doi:10.1016/j.neuroimage.2024.120843.

References

Anderson, A.K., Christoff, K., Stappen, I., Panitz, D., Ghahremani, D.G., Glover, G., Gabrieli, J.D., Sobel, N., 2003. Dissociated neural representations of intensity and valence in human olfaction. Nat. Neurosci. 6, 196–202.

Arshamian, A., Gerkin, R.C., Kruspe, N., Wnuk, E., Floyd, S., O'Meara, C., Garrido Rodriguez, G., Lundstrom, J.N., Mainland, J.D., Majid, A., 2022. The perception of odor pleasantness is shared across cultures. Curr. Biol. 32, 2061-2066 e2063.
Arzi, A., Shedlesky, L., Ben-Shaul, M., Nasser, K., Oksenberg, A., Hairston, I.S., Sobel, N., 2012. Humans can learn new information during sleep. Nat. Neurosci. 15, 1460–1465.
Baccarani, A., Brand, G., Dacremont, C., Valentin, D., Brochard, R., 2021a. The influence of stimulus concentration and odor intensity on relaxing and stimulating perceived properties of odors. Food. Qual. Prefer. 87.
Baccarani, A., Grondin, S., Laflamme, V., Brochard, R., 2021b. Relaxing and stimulating effects of odors on time perception and their modulation by expectancy. Atten. Percept. Psychophys 83, 448–462.
Bensafi, M., Rouby, C., Farget, V., Bertrand, B., Vigouroux, M., Holley, A., 2002. Autonomic nervous system responses to odours: the role of pleasantness and arousal. Chem. Senses. 27, 703–709.
Brand, G., Millot, J.L., 2001. Sex differences in human olfaction: between evidence and enigma. Q. J. Exp. Psychol. B 54, 259–270.
Brody, L.R., Hall, J.A., 2008. Gender and emotion in context. In: Lewis, M., Haviland-Jones, J.M., Barrett, L.F. (Eds.), Handbook of Emotions. Guilford Press, New York, pp. 395–408.
Brookes, M.J., Woolrich, M., Luckhoo, H., Price, D., Hale, J.R., Stephenson, M.C., Barnes, G.R., Smith, S.M., Morris, P.G., 2011. Investigating the electrophysiological basis of resting state networks using magnetoencephalography. Proc. Natl. Acad. Sci. USA 108, 16783–16788.
Buzsaki, G., Draguhn, A., 2004. Neuronal oscillations in cortical networks. Science 304, 1926–1929.
Cereghetti, D., Coppin, G., Porcherot, C., Cayeux, I., Sander, D., Delplanque, S., 2024. Beyond self-report measures of arousal: a new priming task to capture activation of relaxing and energizing feelings elicited by odors. Food. Qual. Prefer. 119, 105227.
Chrea, C., Grandjean, D., Delplanque, S., Cayeux, I., Le Calve, B., Aymard, L., Velazco, M. I., Sander, D., Scherer, K.R., 2009. Mapping the semantic space for the subjective experience of emotional responses to odors. Chem. Senses. 34, 49–62.
Coull, J.T., 1998. Neural correlates of attention and arousal: insights from electrophysiology, functional neuroimaging and psychopharmacology. Prog. Neurobiol. 55, 343–361.
Cunningham, M.O., Pervouchine, D.D., Racca, C., Kopell, N.J., Davies, C.H., Jones, R.S., Traub, R.D., Whittington, M.A., 2006. Neuronal metabolism governs cortical network response state. Proc. Natl. Acad. Sci. USA 103, 5597–5601.
Deacon, D., Shelley-Tremblay, J., 2000. How automatically is meaning accessed: a review of the effects of attention on semantic processing. Front. Biosci. 5, E82–E94.
Deco, G., Jirsa, V.K., McIntosh, A.R., 2013. Resting brains never rest: computational insights into potential cognitive architectures. Trends Neurosci. 36, 268–274.
Doty, R.L., Brugger, W.E., Jurs, P.C., Orndorff, M.A., Snyder, P.J., Lowry, L.D., 1978. Intranasal trigeminal stimulation from odorous volatiles: psychometric responses from anosmic and normal humans. Physiol. Behav. 20, 175–185.
Endo, K., Kazama, H., 2022. Central organization of a high-dimensional odor space. Curr. Opin. Neurobiol. 73, 102528.
Engel, A.K., Gerloff, C., Hilgetag, C.C., Nolte, G., 2013. Intrinsic coupling modes: multiscale interactions in ongoing brain activity. Neuron 80, 867–886.
Flavell, S.W., Gogolla, N., Lovett-Barron, M., Zelikowsky, M., 2022. The emergence and influence of internal states. Neuron 110, 2545–2570.
Gonzalez, J., Barros-Loscertales, A., Pulvermuller, F., Meseguer, V., Sanjuan, A., Belloch, V., Avila, C., 2006. Reading cinnamon activates olfactory brain regions. Neuroimage 32, 906–912.
Gottfried, J.A., 2010. Central mechanisms of odour object perception. Nat. Rev. Neurosci. 11, 628–641.
Goubet, N., Strasbaugh, K., Chesney, J., 2007. Familiarity breeds content? Soothing effect of a familiar odor on full-term newborns. J. Dev. Behav. Pediatr. 28, 189–194.
Hanslmayr, S., Gross, J., Klimesch, W., Shapiro, K.L., 2011. The role of alpha oscillations in temporal attention. Brain Res. Rev. 67, 331–343.
Harris, K.D., Thiele, A., 2011. Cortical state and attention. Nat. Rev. Neurosci. 12, 509–523.
Hyafil, A., Giraud, A.L., Fontolan, L., Gutkin, B., 2015. Neural cross-frequency coupling: connecting architectures, mechanisms, and functions. Trends Neurosci. 38, 725–740.
Jin, J., Zelano, C., Gottfried, J.A., Mohanty, A., 2015. Human amygdala represents the complete spectrum of subjective valence. J. Neurosci. 35, 15145–15156.
Jin, L., Haviland-Jones, J., Simon, J.E., Tepper, B.J., 2018. Influence of aroma intensity and nasal pungency on the 'mood signature' of common aroma compounds in a mixed ethnic population. Food Qual Prefer 65, 164–174.
Joshi, S., Gold, J.I., 2020. Pupil size as a window on neural substrates of cognition. Trends Cogn. Sci. 24, 466–480.
Jovanovic, P., Riera, C.E., 2022. Olfactory system and energy metabolism: a two-way street. Trends Endocrinol. Metab. 33, 281–291.
Klimesch, W., 2012. alpha-band oscillations, attention, and controlled access to stored information. Trends Cogn. Sci. 16, 606–617.
Kret, M.E., Sjak-Shie, E.E., 2019. Preprocessing pupil size data: guidelines and code. Behav Res Methods 51, 1336–1342.
Latora, V., Marchiori, M., 2001. Efficient behavior of small-world networks. Phys. Rev. Lett. 87, 198701.
Laufs, H., Holt, J.L., Elfont, R., Krams, M., Paul, J.S., Krakow, K., Kleinschmidt, A., 2006. Where the BOLD signal goes when alpha EEG leaves. Neuroimage 31, 1408–1418.
Lee, S.H., Dan, Y., 2012. Neuromodulation of brain states. Neuron 76, 209–222.
Lemercier-Talbot, A., Coppin, G., Cereghetti, D., Porcherot, C., Cayeux, I., Delplanque, S., 2019. Measuring automatic associations between relaxing/energizing feelings and odors. Food Qual Prefer 77, 21–31.
Lorig, T.S., Schwartz, G.E., 1988. Brain and odor: I. Alteration of human EEG by odor administration. Psychobiology 16, 281–284.
MacLean, M.H., Arnell, K.M., Cote, K.A., 2012. Resting EEG in alpha and beta bands predicts individual differences in attentional blink magnitude. Brain Cogn. 78, 218–229.
Mainland, J.D., Lundstrom, J.N., Reisert, J., Lowe, G., 2014. From molecule to mind: an integrative perspective on odor intensity. Trends Neurosci. 37, 443–454.
Mantini, D., Perrucci, M.G., Del Gratta, C., Romani, G.L., Corbetta, M., 2007. Electrophysiological signatures of resting state networks in the human brain. Proc. Natl. Acad. Sci. USA 104, 13170–13175.
Marrocco, R.T., Witte, E.A., Davidson, M.C., 1994. Arousal systems. Curr. Opin. Neurobiol. 4, 166–170.
Mathot, S., 2018. Pupillometry: psychology, physiology, and function. J Cogn 1, 16.
McCormick, D.A., Pape, H.C., Williamson, A., 1991. Actions of norepinephrine in the cerebral cortex and thalamus: implications for function of the central noradrenergic system. Prog. Brain Res. 88, 293–305.
Miskovic, V., Anderson, A.K., 2018. Modality general and modality specific coding of hedonic valence. Curr Opin Behav Sci 19, 91–97.
Oostenveld, R., Fries, P., Maris, E., Schoffelen, J.M., 2011. FieldTrip: open source software for advanced analysis of MEG, EEG, and invasive electrophysiological data. Comput. Intell. Neurosci., 156869, 2011.
Ozkurt, T.E., Schnitzler, A., 2011. A critical note on the definition of phase-amplitude cross-frequency coupling. J. Neurosci. Methods 201, 438–443.
Palva, S., Palva, J.M., 2007. New vistas for alpha-frequency band oscillations. Trends Neurosci. 30, 150–158.
Pessoa, L., 2017. A network model of the emotional brain. Trends Cogn. Sci. 21, 357–371.
Pybus, D.H., 2006. The history of aroma chemistry and perfume. In: Sell, C.S. (Ed.), The Chemistry of Fragrances. The Royal Society of Chemistry, pp. 3–23.
Rubinov, M., Sporns, O., 2010. Complex network measures of brain connectivity: uses and interpretations. Neuroimage 52, 1059–1069.
Russell, J.A., 1980. A circumplex model of affect. J. Pers. Soc. Psychol. 39, 1161–1178.
Russell, J.A., 2003. Core affect and the psychological construction of emotion. Psychol. Rev. 110, 145–172.
Schredl, M., Atanasova, D., Hormann, K., Maurer, J.T., Hummel, T., Stuck, B.A., 2009. Information processing during sleep: the effect of olfactory stimuli on dream content and dream emotions. J. Sleep. Res. 18, 285–290.
Schubring, D., Schupp, H.T., 2021. Emotion and brain oscillations: high arousal is associated with decreases in alpha- and lower beta-band power. Cereb. Cortex 31, 1597–1608.
Schwarz, L.A., Miyamichi, K., Gao, X.J., Beier, K.T., Weissbourd, B., DeLoach, K.E., Ren, J., Ibanes, S., Malenka, R.C., Kremer, E.J., Luo, L., 2015. Viral-genetic tracing of the input-output organization of a central noradrenaline circuit. Nature 524, 88–92.
Secundo, L., Snitz, K., Sobel, N., 2014. The perceptual logic of smell. Curr. Opin. Neurobiol. 25, 107–115.
Shapiro, K.L., Raymond, J.E., Arnell, K.M., 1997. The attentional blink. Trends Cogn. Sci. 1, 291–296.
Siebenhuhner, F., Wang, S.H., Arnulfo, G., Lampinen, A., Nobili, L., Palva, J.M., Palva, S., 2020. Genuine cross-frequency coupling networks in human resting-state electrophysiological recordings. PLoS Biol. 18, e3000685.
Siegel, M., Donner, T.H., Engel, A.K., 2012. Spectral fingerprints of large-scale neuronal interactions. Nat. Rev. Neurosci. 13, 121–134.
Soussignan, R., Schaal, B., Marlier, L., Jiang, T., 1997. Facial and autonomic responses to biological and artificial olfactory stimuli in human neonates: re-examining early hedonic discrimination of odors. Physiol. Behav. 62, 745–758.
Steriade, M., 2006. Grouping of brain rhythms in corticothalamic systems. Neuroscience 137, 1087–1106.
Stitt, I., Zhou, Z.C., Radtke-Schuller, S., Frohlich, F., 2018. Arousal dependent modulation of thalamo-cortical functional interaction. Nat. Commun. 9, 2455.
Thomas, L., 1990. A Long Line of cells. Book-of-the-Month Club.
Valdez, P., Mehrabian, A., 1994. Effects of color on emotions. J. Exp. Psychol. Gen. 123, 394–409.
Vidaurre, D., Hunt, L.T., Quinn, A.J., Hunt, B.A.E., Brookes, M.J., Nobre, A.C., Woolrich, M.W., 2018. Spontaneous cortical activity transiently organises into frequency specific phase-coupling networks. Nat. Commun. 9, 2987.
Vinck, M., van Wingerden, M., Womelsdorf, T., Fries, P., Pennartz, C.M., 2010. The pairwise phase consistency: a bias-free measure of rhythmic neuronal synchronization. Neuroimage 51, 112–122.
Vul, E., Nieuwenstein, M., Kanwisher, N., 2008. Temporal selection is suppressed, delayed, and diffused during the attentional blink. Psychol. Sci. 19, 55–61.
Watts, D.J., Strogatz, S.H., 1998. Collective dynamics of 'small-world' networks. Nature 393, 440–442.
Winston, J.S., Gottfried, J.A., Kilner, J.M., Dolan, R.J., 2005. Integrated neural representations of odor intensity and affective valence in human amygdala. J. Neurosci. 25, 8903–8907.
Womelsdorf, T., Valiante, T.A., Sahin, N.T., Miller, K.J., Tiesinga, P., 2014. Dynamic circuit motifs underlying rhythmic gain control, gating and integration. Nat. Neurosci. 17, 1031–1039.
Wysocki, C.J., Cowart, B.J., Radil, T., 2003. Nasal trigeminal chemosensitivity across the adult life span. Percept. Psychophys. 65, 115–122.
Zhou, Y., Smith, B.H., Sharpee, T.O., 2018. Hyperbolic geometry of the olfactory space. Sci. Adv. 4, eaaq1458.